ACS Synthetic Biology
Cite This: ACS Synth. Biol. 2018, 7, 2790−2795
Letter
pubs.acs.org/synthbio

Cell-Based Biosensor with Dual Signal Outputs for Simultaneous Quantification of Phenylacetic Acid and Phenylethylamine

Kai-Hong Guo, Kun-Hua Lu, and Yi-Chun Yeh*

Department of Chemistry, National Taiwan Normal University, 88, Section 4, Tingzhou Road, Taipei 11677, Taiwan

Supporting Information

ABSTRACT: Despite the importance of 2-phenylacetic acid, a plant hormone in the endogenous auxin family, its biosynthesis pathway has yet to be elucidated. In this study, we developed a novel whole-cell biosensor for the simultaneous quantification of 2-phenylacetic acid (PA) and 2-phenylethylamine (PEA) through the regulation of bacterial catabolism of aromatic compounds. We used the PA regulon to enable the recognition of PA and PEA. Differentiation of PEA from PA involves the incorporation of the FeaR regulon within the same whole-cell biosensor to report the presence of aromatic amines. The proposed system is highly sensitive to PA as well as PEA.

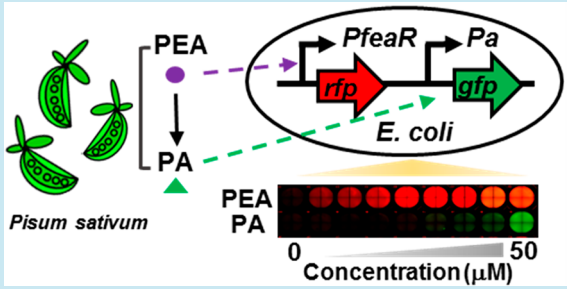

KEYWORDS: *phenylacetic acid, phenylethylamine, auxin, E. coli, aromatic acids, FeaR regulon*

The temporal and spatial regulation of the plant's growth cycle according to auxin levels ensures that cell division and elongation are tightly coordinated with other physical processes.[1] In addition, the level and gradient distribution of auxin in plants is crucial to the regulation of organogenesis.[2−4] There are two types of auxin action-mechanisms: rapid cellular auxin effects mediated by Auxin Binding Protein 1 (ABP1)[5] and developmental outputs triggered by auxin-dependent transcriptional regulations.[6] Indole-3-acetic acid (IAA) is the most studied and abundant endogenous auxin.[7] The biological activity of 2-phenylacetic acid (PA), the only phenyl-derivative endogenous auxins, is weaker than that of IAA; however, it can be found in a wide range of plant species.[8,9] Previous studies have suggested that PA plays a role in the interactions of plant roots with soil microorganisms.[10]

The biosynthesis of PA in plants has yet to be fully elucidated. Recent studies on *Pisum sativum* suggest that PA is synthesized from the phenylalanine *via* phenylpyruvate;[11] however, the phenylalanine-derived volatile compound (2-phenylethanol, 2-PE) involves the conversion of phenylalanine into 2-phenethylamine (PEA) by decarboxylases as an intermediate.[12] This means the ability to monitor PEA (the decarboxylation product of phenylalanine) and PA simultaneously may be beneficial to the study of PA biosynthesis.[13] The quantification of auxin for horticulture purposes requires rapid and sensitive analysis of plant tissues, soil, and environmental aqueous samples. The analytical methods, such as liquid chromatography in combination with ESI-mass spectrometry (LC−ESI-MS),[14] GC−MS,[15] and isocratic reversed-phase HPLC with precolumn derivatization were developed for the quantification of auxin;[16] however, these methods require expensive instruments and highly specialized technicians. The molecule-based or cell-based biosensors have attracted a lot of research effort and have been used in environmental monitoring and clinical diagnostics.[17−23] Dierckx et al. recently developed a whole-cell biosensor for the detection of environmental auxin based on bacterial *hpa* regulon;[24] however, it responded to both PA and its hydroxylated derivatives. Consequently, our primary objective in this study was to develop a method for the simple, rapid, and sensitive detection and differentiation of PA and PEA *via* bacterial catabolic regulons.

In *E. coli*, the catabolism of PEA to phenylacetaldehyde (PAL) is catalyzed by the periplasmic amine oxidase (TynA). The resulting PAL is subsequently oxidized to PA *via* FeaB (PAL dehydrogenase) (Scheme 1A).[25,26] In the catabolism of aromatic amines (including PEA, tyramine, and dopamine), the expression of TynA and FeaB is activated by FeaR regulon during carbon or nitrogen limitation.[27,28] FeaR is a member of the AraC family of activators, and involved in catabolism of aromatics in *E. coli* for the oxidative deamination of monoamines to the corresponding aldehyde, hydrogen peroxide, and ammonia. In contrast, PA catabolism is regulated by two genes, *paaX* and *paaY*, that form an operon driven by the *Px* promoter. PaaX protein acts as a transcriptional repressor toward *Px*, *Pa*, and *Pz* promoters. However, the binding of PaaX to promoters *Px*, *Pa*, and *Pz* is inhibited in the presence of PA-CoA,[29,30] the process of which is catalyzed through CoA thioesterification by the PA-CoA ligase (PaaK); next, PA-CoA binds to PaaX and inhibits its repression (Scheme 1B). In this study, we therefore used the PA regulon to enable the recognition of PA and PEA since the activity of green fluorescent protein (GFP) reporter depends the presence of PA (conversion of PEA to PA resulting the activation of GFP as well). In addition, we designed our

Received: October 2, 2018
Published: November 12, 2018

DOI: 10.1021/acssynbio.8b00416
ACS Synth. Biol. 2018, 7, 2790−2795

Scheme 1. Schematic Representations of (A) Biochemistry of PEA Catabolic Pathway and (B) the Regulations of FeaR and PA Regulons[a]

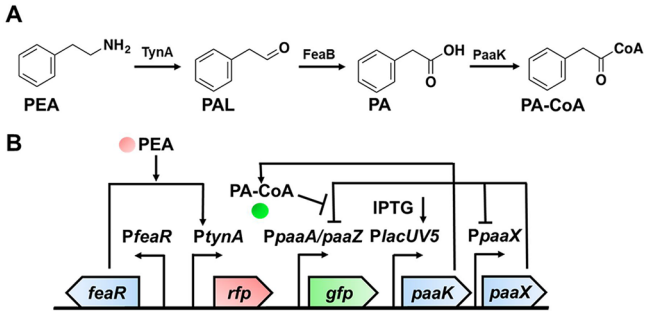

[a]For PA regulon: PaaX represses PaaA/Z/X promoters, while PaaK induces PA-CoA. Next, PA-CoA binds to PaaX to inhibit its repression. FeaR regulon is activated in the presence of primary amines.

biosensor by using PEA to activate FeaR-regulating promoters, which were activated in the presence of aromatic amines to induce the expression of red fluorescent protein (RFP). Thus, differentiation of PEA from PA involves the incorporation of the FeaR regulon within a whole-cell biosensor to report the presence of aromatic amines (Scheme 1B).

We examined the induction of *Pa* and *Pz* promoters in the presence of PA with or without the expression of PaaK and PaaX. Four strains carrying various plasmids (Figure S1A) were constructed, including *Pa/Pz-gfp* with or without *PlacUV5-paaKX*. Sensor cells were grown in modified M9 minimal medium supplemented with 2% glycerol to avoid the repression effect of glucose that was observed for transcriptional activation of the *paa* operons.[29] Figure S1B presents a comparison of the end points GFP intensity/OD_{600} and OD_{600} values in the cells in the presence of PA at 500 μM and 100 μM of IPTG for 24 h. Among four strains, two strains with the coexpression of PaaK and PaaX showed the PA-dependent induction. YCY844 (carrying *Pa-gfp*) and YCY845 (carrying *Pz-gfp*) presented a 10.7 and 2.7-fold increase in fluorescence intensity compared to those without the presence of PA. Nonetheless, strains without additional copies of PaaK and PaaX on plasmid did not show significant induction in the presence of PA. Thus, YCY844 was used in all subsequent tests through this study. However, cells showed slightly lower cell density (OD_{600} values) due to overexpression of *paaK*.

The selectivity of the proposed sensor was evaluated by screening various substrates at 500 μM for 24 h in the presence of 100 μM of IPTG. Specifically, the hydroxylated derivatives of PA were examined to understand the cross-talk between PaaX and HpaR-mediated regulations due to the structural similarities of their substrates. Sixteen compounds were tested including three hydroxylated derivatives (4-hydroxyphenylacetic acid (4-HPA), 2-hydroxyphenylacetic acid (2-HPA), 3,4-dihydroxyphenylacetic acid), IAA (most abundant auxin), phenylpyruvic acid (intermediate of phenylalanine metabolism), 2-PE, and various aromatic acids structure analogues (mandelic acid, benzoic acid, salicylic acid, 4-hydroxybenzoic acid, 3-aminobenzoic acid, 4-aminobenzoic acid, 3,5-dimethoxybenzoic acid, 4-methoxyphenylacetic acid, *p*-anisic acid, and 2,4,6-trimethylbenzoic acid). Figure 1A illustrates the chemical structures of 16 compounds used in the discrimination of PA, whereupon the end-point fluorescence intensity/OD_{600} ratio of sensor cells in the presence of various substrates at 500 μM for 24 h was compared. Note that GFP fluorescence intensity increased significantly in the presence of PA (Figure 1B), whereas other compounds did not induce the GFP fluorescence. The hydroxylated derivatives 1 (4-HPA), 2 (2-HPA), and 6 (2-PE) slightly induced the expression of GFP.

The proposed biosensor presented a high degree of sensitivity specifically to PA. We then optimized the conditions for sensing based on the kinetics of GFP expression in the sensor strain. A detectable response was produced after incubating the cells in the presence of 500 μM PA for 3 h (Figure S2A), and peak induction levels were observed after 12 h. In all subsequent experiments, incubation was conducted at 5 h to enable rapid detection with reasonable incubation. Next, we measured the GFP fluorescence intensity/OD_{600} ratio of sensor cells from 5 h postinduction in the presence of PA, 2-HPA, 2-PE, and 4-HPA at concentrations ranging from 0.5 to 1000 μM and 100 μM of IPTG. Our results revealed that PA induces GFP at concentrations as low as 10 μM, and the response reached saturation at a concentration of approximately 200 μM. GFP intensities of 2-HPA/4-HPA/2-PE were significantly lower than those of PA (Figure 2), which indicates the interference from these three substrates should be negligible. Michaelis–Menten fitting curve and constants between green fluorescence intensity/OD_{600} and PA concen-

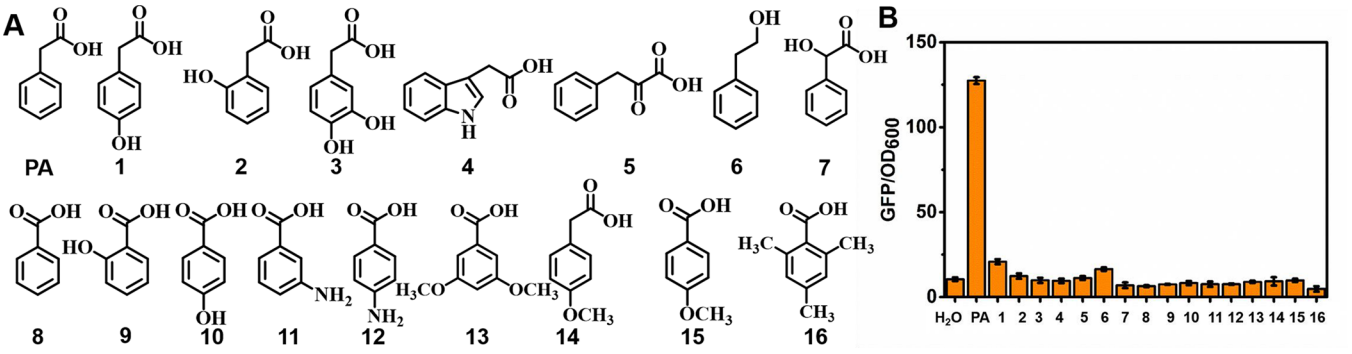

Figure 1. Selectivity of the proposed sensor. (A) Chemical structures of the investigated substrates, including (1) 4-HPA, (2) 2-HPA, (3) 3,4-dihydroxyphenylacetic acid, (4) IAA, (5) phenylpyruvic acid, (6) 2-PE, (7) mandelic acid, (8) benzoic acid, (9) salicylic acid, (10) 4-hydroxybenzoic acid, (11) 3-aminobenzoic acid, (12) 4-aminobenzoic acid, (13) 3,5-dimethoxybenzoic acid, (14) 4-methoxyphenylacetic acid, (15) *p*-anisic acid, and (16) 2,4,6-trimethylbenzoic acid. (B) The end-point fluorescence intensity/OD_{600} ratios of sensor cells in the presence of 100 μM of IPTG and various substrates at 500 μM for 24 h.

DOI: 10.1021/acssynbio.8b00416
ACS Synth. Biol. 2018, 7, 2790–2795

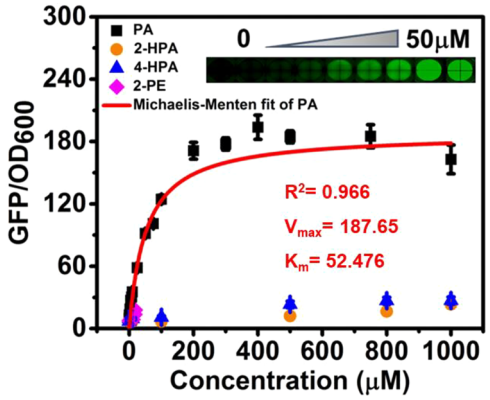

Figure 2. Dose−response curves of sensor cells in the presence of 100 μM of IPTG and PA, 2-HPA, 4-HPA, or 2-PE from 5 h postinduction. Michaelis−Menten constants and fitting between GFP/OD_{600} and various concentrations of PA were presented. Insets: the fluorescence photograph of GFP in the presence of PA.

trations was shown in Figure 2. Fluorescence photograph of a 96-well plate containing sensor cells with various concentrations of PA from 5 h postinduction was presented in the inset of Figure 2. The cell growth condition (OD_{600} values) was presented to examine the toxicity of the substrates on the sensor cells in Figure S2B. The toxicity of exposure to PA or PEA was not detected at concentrations less than 200 μM. In addition, the GFP fluorescence intensity/OD_{600} was compared to understand effects of varying the IPTG level (tuning PaaK) (Figure S2C). Interestingly, the intensities of GFP fluorescence were similar even in the absence of IPTG. This result could be that negative-feedback control of PaaX minimized its expression (a lower PaaX level requires less PA-CoA for regulation). Thus, the basal level of PaaK is enough for the activation of *Pa*.

To enable the simultaneous quantification of PEA (in addition to PA), we introduced the FeaR regulon to report the presence of primary amines in the same strain (YCY877, Figure S1A). Performance of the two-regulon system was evaluated using a standard addition method to derive the dose−response curves of the four substrates including PA, PEA, dopamine (DA), and L-DOPA (Figure 3A−D) in the presence of 100 μM IPTG from 5 h postinduction. The OD_{600} values were presented in Figure S2D to examine the toxicity of four substrates. DA and L-DOPA were examined as control groups (positive and negative control) to validate the specificity of current sensors, because DA is known to be the substrates of the FeaR regulon.[28] PA and PEA were shown to induce GFP. PEA and DA produced an increase in RFP, whereas L-DOPA did not promote the expression of GFP or RFP (Figure 3D). The Michaelis−Menten fitting curves between fluorescence intensity and substrate concentrations, R^2, and fitting constants were shown in Figure 3A−C. Supplementing the growth medium with PEA led to an increase of green and red fluorescence intensity values at the single-cell level (Figure S3). Notably, fluorescence microscopy images obtained at the single-cell-level in the presence of four substrates were consistent with the results of ensemble analysis (Figure 3E).

We then added PEA and PA to the growth media to determine whether the coexistence of two compounds (i.e., the presence of two inducers) would cause interference. GFP and RFP fluorescence intensity heat maps of PA and PEA from 5 h postinduction were presented in Figure S4A,B; the fluorescence intensities of GFP in the mixtures remained the same in the presence or absence of PEA (when PEA less than 10 μM). Similar fluorescence intensities of RFP were observed in the presence or absence of PA (Figure S4B), suggesting that the coexistence of PA did not cause interferences toward FeaR regulon. These results may be attributed to the fact that the conversions of PA from PEA (PA: final products of PEA catabolisms) at the low concentrations were little. However, the presence of a high amount of PEA (25 and 50 μM) does cause interference of the GFP intensity for reporting the level of PA. Therefore, the level of RFP could be used to determine

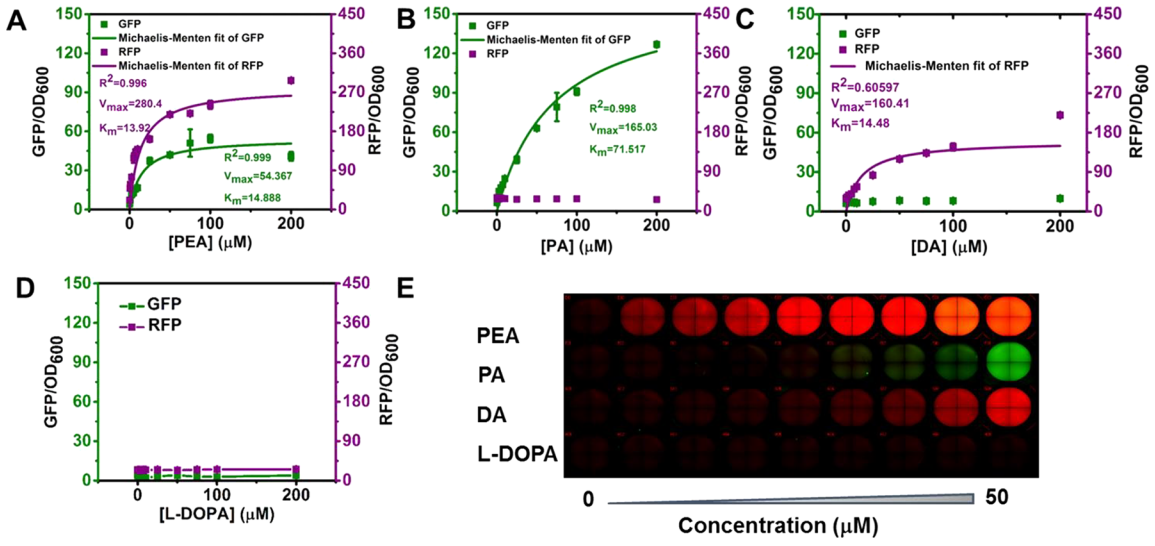

Figure 3. Dose−response curves of two-regulon sensor cells from 5 h postinduction in the presence of (A) PEA, (B) PA, (C) DA, and (D) L-DOPA. Michaelis−Menten constants and fittings between GFP or RFP/OD_{600} and various concentrations of (A) PEA, (B) PA, and (C) DA were presented. (E) Overlay of red and green fluorescence photograph in the presence of four substrates at various concentrations from 5 h postinduction.

DOI: 10.1021/acssynbio.8b00416
ACS Synth. Biol. 2018, 7, 2790−2795

the concentrations of PEA to select appropriate pretreatment steps for the quantifications of PA.

The interference effect of coexisting DA was examined because it has been found in many plants. Figure S5A,B showed the RFP and GFP fluorescence intensity/OD_{600} from 5 h postinduction supplemented with DA alone or mixture of DA and PEA. Interesting, the presence of DA (up to 25 μM) did not interfere with the intensities of both RFP and GFP fluorescence. Specifically, it has been reported that the average concentration of DA is usually low in plants except for that in the pulp of bananas.[31] Thus, the effect of DA can be considered negligible.

The applications of the proposed sensor were evaluated for the determination of PA and PEA in the analysis of environmental samples to understand the effects of a complicated sample matrix. Pond water samples were first diluted with 2XM9 for the cell-based analyses. Samples presented undetectable values of both PA and PEA. We therefore spiked with various concentrations of PA and PEA in the presence of 100 μM IPTG, and examined the fluorescence intensity/OD_{600} from 5 h postinduction. The fluorescence intensity/OD_{600} of pond water and pure water for PA and PEA were almost identical, respectively (Figure 4). This result suggests that the proposed sensor has great potential for the sensing of PA and PEA in environmental samples.

In summary, we used two catabolic regulons to construct a whole-cell biosensor for the simultaneous quantification of PA and PEA. The proposed system presents great specificity and sensitivity for the analysis of environmental samples. The cost of the cell-based sensor is extremely low compared to conventional analytical systems, but to improve this further it has been shown that cells can be embedded in a portable system including paper[32,33] or sol−gel[34,35] to develop a miniaturized platform. Specifically, not only do these two molecules play important roles in the development of plants but also, interestingly, stress has been shown to alter the level of PEA and PA in the central and peripheral nervous system of humans.[36] As tools for genetic engineering continue to develop, we envision that it will be possible to improve the current system which is suitable for point-of care settings and can provide the diagnosis information. A subsequent investigation of reducing carbon catabolite repression from glucose will broaden the applicability of the proposed sensors in human specimens.

MATERIALS AND METHODS

Bacteria Growth Conditions. Cells were grown in lysogeny broth (LB) medium at 37 °C overnight, and diluted in LB:M9 at a ratio of 1:25. The M9 medium was supplemented with 2% glycerol (Amresco), 0.24 mg/mL $MgSO_4$ (Fisher chemical), 11.1 μg/mL $CaCl_2$ (Ferak Berlin GmbH), and 5 mg/mL thiamine hydrochloride (Sigma-Aldrich). Both the LB and M9 media were supplemented with 50 μg/mL of kanamycin (Amresco), and 100 μg/mL chloramphenicol (Amresco) and appropriate concentrations of isopropyl β-D-1-thiogalactopyranoside (IPTG) (Amresco).

Plasmids and Bacterial Strains. Plasmids, bacterial strains, and primers used in this work are listed in Tables S1, S2, and S3. The construction details are provided in Table S2. All plasmids were confirmed by DNA sequencing.

Preparation of PEA/PA/DA/L-DOPA Solutions. 2-Phenylethylamine (PEA) (Sigma-Aldrich), and phenylacetic acid (PA) (Sigma-Aldrich) were dissolved in ethanol (Fisher ACS grade, 99.5%). Dopamine (Acros Organics), and L-DOPA (Acros Organics) were freshly prepared in double-distilled water (Milli-Q purification system).

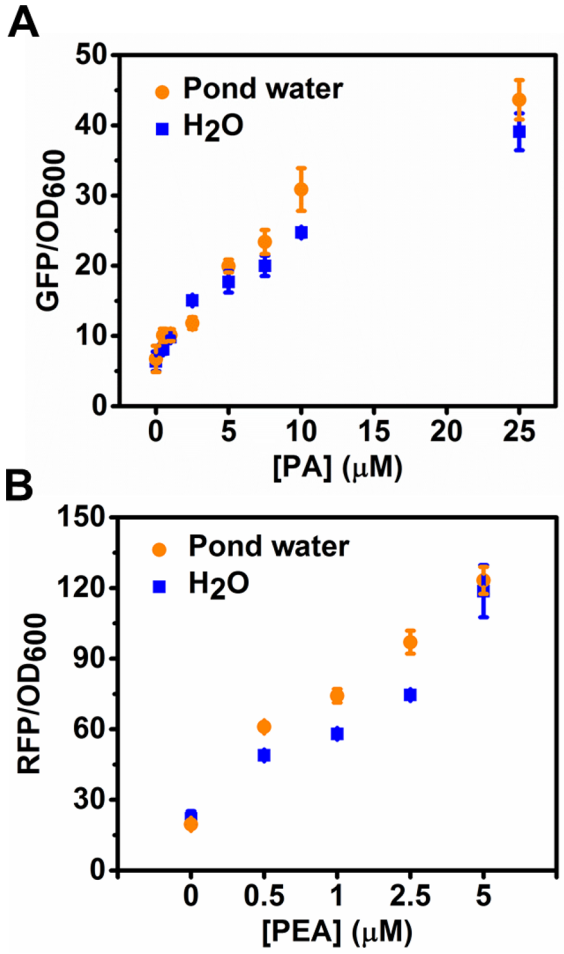

Figure 4. GFP or RFP/OD_{600} of two-regulon sensor cells in response to (A) PA and (B) PEA at various concentrations and 100 μM of IPTG from 5 h postinduction in pure and pond water samples. Error bars represent the standard deviation from triplicate measurements.

Comparisons of Various Sensor Strains. Cell cultures were incubated at 37 °C until OD_{600} reaching early exponential phase ~0.4 and then split into "control" and "induced" groups. Phenylacetic acid was used to induce the expression of GFP fluorescence. For strain YCY844 and YCY845, 100 μM IPTG was added in the cultures for the expression of the protein of PaaK and PaaX. All measurements were performed with three biological replicates. The quantitation of OD_{600}/GFP intensity was recorded at the indicated time points.

GFP and RFP Intensity Quantifications. After induction with substrates, 300 μL of cell cultures were centrifuged (14 000 rpm, 2 min). The cell pellets were washed and resuspended in 300 μL of PBS buffer, and then transferred to a microplate. The OD_{600}, RFP intensity (excitation/emission filters: 530 nm/590 nm), and GFP intensity (excitation/emission filters: 485 nm/528 nm) were measured by a microplate reader BioTek Synergy HT (BioTek, Winooski, VT). The error bars represent the standard deviation from three independent measurements.

Specificity of Sensor Strain toward Various Substrates. The cells were grown as mentioned above. The substrates including PA, 2-hydroxyphenylacetic acid (Acros

DOI: 10.1021/acssynbio.8b00416
ACS Synth. Biol. 2018, 7, 2790−2795

Organics), 4-hydroxyphenylacetic acid (Acros Organics), 3,4-dihydroxyphenylacetic acid, benzoic acid (Acros Organics), salicylic acid (Acros Organics), 3-aminobenzoic acid (Acros Organics), 4-aminobenzoic acid (Acros Organics), *p*-hydroxybenzoic acid (Hayashi), mandelic acid (Acros Organics), 4-methoxyphenylacetic acid (Acros Organics), 3,5-dimethoxybenzoic acid (Acros Organics), *p*-anisic acid (Sigma-Aldrich), 2,4,6-trimethylbenzoic acid (Fluka), indole-3-acetic acid (Sigma-Aldrich)), and 2-phenylethanol (Acros Organics) were used to examine the specificity of the biosensor.

Preparation of Environmental Samples. Pond water samples were collected from National Taiwan Normal University ecological pond. Samples were centrifuged (room temperature, 9000 rpm, 10 min) to remove the precipitation before use. Then pond water was mixed with 2X M9 at a ratio of 1:1 as our culture medium. PEA and PA were spiked in medium with standard addition methods.

Fluorescence Microscopy. Cells were grown in the presence of PEA, PA, DA, and L-DOPA (50 μM), and were immobilized on a thin layer of 1% agarose in PBS medium. Phase contrast and fluorescence microscopy images were obtained using a Zeiss Axio A1Microscope with an EC Plan-Neofluar 100*x*/1.30, and oil PH3 objective.

■ ASSOCIATED CONTENT

Supporting Information

The Supporting Information is available free of charge on the ACS Publications website at DOI: 10.1021/acssynbio.8b00416.

Experimental details and RFP/GFP characterizations (PDF)

■ AUTHOR INFORMATION

Corresponding Author

*Tel.: +886277346117. Fax:+886229324249. E-mail: yichuny@ntnu.edu.tw.

ORCID

Yi-Chun Yeh: 0000-0002-8267-0360

Notes

The authors declare no competing financial interest.

■ ACKNOWLEDGMENTS

This work was funded by the Ministry of Science and Technology of Taiwan under the Project No. 105-2113-M-003-013-MY2 and 107-2113-M-003-013-MY3. We thank Molecular Imaging Core Facility of National Taiwan Normal University for the assistance in high-content fluorescence microscopes.

■ REFERENCES

(1) Perrot-Rechenmann, C. (2010) Cellular Responses to Auxin: Division versus Expansion. *Cold Spring Harbor Perspect. Biol. 2*, a001446.

(2) Pernisova, M., Klima, P., Horak, J., Valkova, M., Malbeck, J., Soucek, P., Reichman, P., Hoyerova, K., Dubova, J., Friml, J., Zazimalova, E., and Hejatko, J. (2009) Cytokinins Modulate Auxin-Induced Organogenesis in Plants via Regulation of the Auxin Efflux. *Proc. Natl. Acad. Sci. U. S. A. 106*, 3609−3614.

(3) Vanneste, S., and Friml, J. (2009) Auxin: A Trigger for Change in Plant Development. *Cell 136*, 1005−1016.

(4) Petrasek, J., and Friml, J. (2009) Auxin Transport Routes in Plant Development. *Development 136*, 2675−2688.

(5) Tromas, A., Braun, N., Muller, P., Khodus, T., Paponov, I. A., Palme, K., Ljung, K., Lee, J.-Y., Benfey, P., Murray, J. A. H., Scheres, B., and Perrot-Rechenmann, C. (2009) The Axin Binding Protein 1 Is Required for Differential Auxin Responses Mediating Root Growth. *PLoS One 4*, No. e6648.

(6) Walker, L., and Estelle, M. (1998) Molecular Mechanisms of Auxin Action. *Curr. Opin. Plant Biol. 1*, 434−439.

(7) Spaepen, S., Vanderleyden, J., and Remans, R. (2007) Indole-3-Acetic Acid in Microbial and Microorganism-Plant Signaling. *FEMS Microbiol. Rev. 31*, 425−448.

(8) Frank, W., and L, L. D. (1982) Identification of Phenylacetic Acid as a Natural Auxin in the Shoots of Higher Plants. *Physiol. Plant. 55*, 17−24.

(9) Schneider, E. A., Kazakoff, C. W., and Wightman, F. (1985) Gas Chromatography-Mass Spectrometry Evidence for Several Endogenous Auxins in Pea Seedling Organs. *Planta 165*, 232−241.

(10) Spaepen, S., and Vanderleyden, J. (2011) Auxin and Plant-Microbe Interactions. *Cold Spring Harbor Perspect. Biol. 3*, a001438.

(11) Sugawara, S., Mashiguchi, K., Tanaka, K., Hishiyama, S., Sakai, T., Hanada, K., Kinoshita-Tsujimura, K., Yu, H., Dai, X., Takebayashi, Y., Takeda-Kamiya, N., Kakimoto, T., Kawaide, H., Natsume, M., Estelle, M., Zhao, Y., Hayashi, K.-i., Kamiya, Y., and Kasahara, H. (2015) Distinct Characteristics of Indole-3-Acetic Acid and Phenylacetic Acid, Two Common Auxins in Plants. *Plant Cell Physiol. 56*, 1641−1654.

(12) Kaminaga, Y., Schnepp, J., Peel, G., Kish, C. M., Ben-Nissan, G., Weiss, D., Orlova, I., Lavie, O., Rhodes, D., Wood, K., Porterfield, D. M., Cooper, A. J. L., Schloss, J. V., Pichersky, E., Vainstein, A., and Dudareva, N. (2006) Plant Phenylacetaldehyde Synthase Is a Bifunctional Homotetrameric Enzyme That Catalyzes Phenylalanine Decarboxylation and Oxidation. *J. Biol. Chem. 281*, 23357−23366.

(13) Cook, S. D., Nichols, D. S., Smith, J., Chourey, P. S., McAdam, E. L., Quittenden, L., and Ross, J. J. (2016) Auxin Biosynthesis: Are the Indole-3-Acetic Acid and Phenylacetic Acid Biosynthesis Pathways Mirror Images? *Plant Physiol. 171*, 1230−1241.

(14) Cao, J., Murch, S. J., O'Brien, R., and Saxena, P. K. (2006) Rapid Method for Accurate Analysis of Melatonin, Serotonin and Auxin in Plant Samples Using Liquid Chromatography−Tandem Mass Spectrometry. *J. Chromatogr. A 1134*, 333−337.

(15) Cohen, J. D., Baldi, B. G., and Slovin, J. P. (1986) (13)C(6)-[Benzene Ring]-Indole-3-Acetic Acid: A New Internal Standard for Quantitative Mass Spectral Analysis of Indole-3-Acetic Acid in Plants. *Plant Physiol. 80*, 14−19.

(16) Dobrev, P. I., Havlíček, L., Vágner, M., Malbeck, J., and Kamínek, M. (2005) Purification and Determination of Plant Hormones Auxin and Abscisic Acid Using Solid Phase Extraction and Two-Dimensional High Performance Liquid Chromatography. *J. Chromatogr. A 1075*, 159−166.

(17) Bereza-Malcolm, L. T., Mann, G., and Franks, A. E. (2015) Environmental Sensing of Heavy Metals Through Whole Cell Microbial Biosensors: A Synthetic Biology Approach. *ACS Synth. Biol. 4*, 535−546.

(18) Chong, H., and Ching, C. B. (2016) Development of Colorimetric-Based Whole-Cell Biosensor for Organophosphorus Compounds by Engineering Transcription Regulator DmpR. *ACS Synth. Biol. 5*, 1290−1298.

(19) Harbaugh, S. V., Goodson, M. S., Dillon, K., Zabarnick, S., and Kelley-Loughnane, N. (2017) Riboswitch-Based Reversible Dual Color Sensor. *ACS Synth. Biol. 6*, 766−781.

(20) Watstein, D. M., and Styczynski, M. P. (2018) Development of a Pigment-Based Whole-Cell Zinc Biosensor for Human Serum. *ACS Synth. Biol. 7*, 267−275.

(21) Lin, Y.-K., and Yeh, Y.-C. (2017) Dual-Signal Microbial Biosensor for the Detection of Dopamine without Inference from Other Catecholamine Neurotransmitters. *Anal. Chem. 89*, 11178−11182.

(22) Tseng, H.-W., Tsai, Y.-J., Yen, J.-H., Chen, P.-H., and Yeh, Y.-C. (2014) A Fluorescence-Based Microbial Sensor for the Selective Detection of Gold. *Chem. Commun. 50*, 1735−1737.

DOI: 10.1021/acssynbio.8b00416
ACS Synth. Biol. 2018, 7, 2790−2795

(23) Han, J., Wang, B., Bender, M., Seehafer, K., and Bunz, U. H. F. (2016) Water-Soluble Poly(p-aryleneethynylene)s: A Sensor Array Discriminates Aromatic Carboxylic Acids. *ACS Appl. Mater. Interfaces 8*, 20415−20421.
(24) Dierckx, S., Van Puyvelde, S., Venken, L., Eberle, W., and Vanderleyden, J. (2015) Design and Construction of a Whole Cell Bacterial 4-Hydroxyphenylacetic Acid and 2-Phenylacetic Acid Bioassay. *Front. Bioeng. Biotechnol. 3*, 88.
(25) Teufel, R., Mascaraque, V., Ismail, W., Voss, M., Perera, J., Eisenreich, W., Haehnel, W., and Fuchs, G. (2010) Bacterial Phenylalanine and Phenylacetate Catabolic Pathway Revealed. *Proc. Natl. Acad. Sci. U. S. A. 107*, 14390−14395.
(26) Prieto, M. A., Galan, B., Torres, B., Ferrandez, A., Fernandez, C., Minambres, B., Garcia, J. L., and Diaz, E. (2004) Aromatic Metabolism versus Carbon Availability: the Regulatory Network That Controls Catabolism of Less-Preferred Carbon Sources in Escherichia coli. *FEMS Microbiol. Rev. 28*, 503−518.
(27) Zeng, J., and Spiro, S. (2013) Finely Tuned Regulation of the Aromatic Amine Degradation Pathway in Escherichia coli. *J. Bacteriol. 195*, 5141−5150.
(28) Diaz, E., Ferrandez, A., Prieto, M. A., and Garcia, J. L. (2001) Biodegradation of Aromatic Compounds by Escherichia coli. *Microbiol. Mol. Biol. Rev. 65*, 523−569.
(29) Ferrández, A., García, J. L., and Díaz, E. (2000) Transcriptional Regulation of the Divergent paa Catabolic Operons for Phenylacetic Acid Degradation in Escherichia coli. *J. Biol. Chem. 275*, 12214−12222.
(30) Ferrandez, A., Minambres, B., Garcia, B., Olivera, E. R., Luengo, J. M., Garcia, J. L., and Diaz, E. (1998) Catabolism of Phenylacetic Acid in Escherichia coli. Characterization of a New Aerobic Hybrid Pathway. *J. Biol. Chem. 273*, 25974−25986.
(31) Kulma, A., and Szopa, J. (2007) Catecholamines are active compounds in plants. *Plant Sci. 172*, 433−440.
(32) Struss, A., Pasini, P., Ensor, C. M., Raut, N., and Daunert, S. (2010) Paper strip whole cell biosensors: a portable test for the semiquantitative detection of bacterial quorum signaling molecules. *Anal. Chem. 82* (11), 4457−4463.
(33) Guo, K. H., Chen, P. H., Lin, C., Chen, C. F., Lee, I. R., and Yeh, Y. C. (2018) Determination of Gold Ions in Human Urine Using Genetically Engineered Microorganisms on a Paper Device. *ACS sensors 3* (4), 744−748.
(34) Carturan, G., Dal Toso, R., Boninsegna, S., and Dal Monte, R. (2004) Encapsulation of functional cells by sol−gel silica: actual progress and perspectives for cell therapy. *J. Mater. Chem. 14* (14), 2087−2098.
(35) Premkumar, J. R., Sagi, E., Rozen, R., Belkin, S., Modestov, A. D., and Lev, O. (2002) Fluorescent Bacteria Encapsulated in Sol− Gel Derived Silicate Films. *Chem. Mater. 14* (6), 2676−2686.
(36) Paulos, M., Mosnaim, A., Wolf, M., and Tessel, R. (1984) Phenylethylamine, Phenylacetic Acid and Methionine Enkephalin Levels in Humans Following Profound Acute Stress. *Neurobiology of the Trace Amines*; Springer, pp 563−569 DOI: 10.1007/978-1-4612-5312-9_49.

DOI: 10.1021/acssynbio.8b00416
ACS Synth. Biol. 2018, 7, 2790−2795